

# Proprioception Is All You Need: Terrain Classification for Boreal Forests

Damien LaRocque<sup>1</sup> William Guimont-Martin<sup>1</sup>  
David-Alexandre Duclos<sup>1</sup> Philippe Giguère<sup>1</sup> François Pomerleau<sup>1</sup>

<sup>1</sup>Northern Robotics Laboratory, Université Laval, Quebec City, Canada

Friday 18<sup>th</sup> October, 2024



# WhoAml

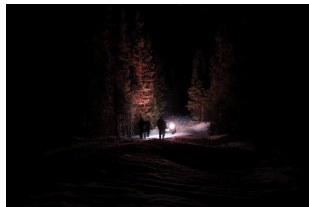
Damien LaRocque

- ▶ B.Eng (Electrical), Université de Moncton, 2020
- ▶ M.Sc. Computer Science, Université Laval, 2024



# Northern Robotics Laboratory

Field deployments in *Forêt Montmorency*



# Northern Robotics Laboratory

Challenging terrains in *Forêt Montmorency*



(a) In deep snow



(b) In peat moss

Figure 1: Issues encountered during autonomous driving experiments



# Overview

Context and motivations

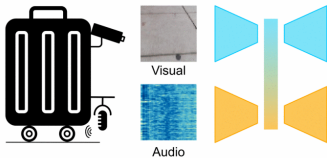
Methodology

Results

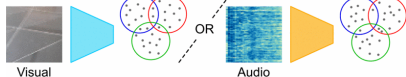
Conclusion

# Context

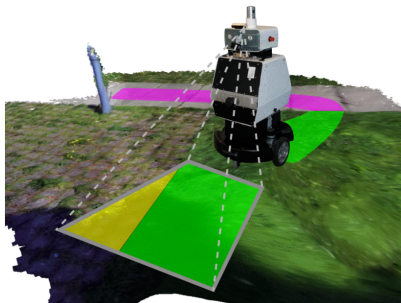
## Training



## Testing



(a) Ishikawa *et al.* [1]



(b) Zürn *et al.* [2]

Figure 2: Audiovisual-based terrain classification (TC)

# Context

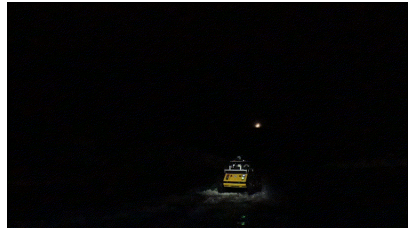
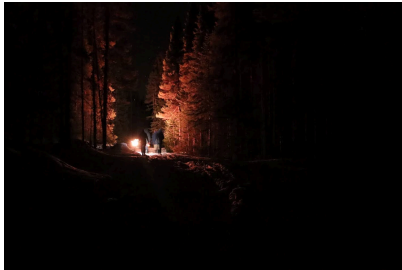
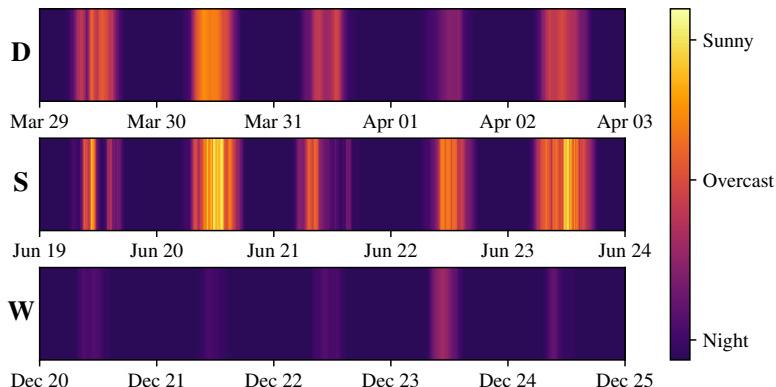


Figure 3: Dark conditions in *Forêt Montmorency*

# Context



**Figure 4:** Hourly sun radiation measurements in *Forêt Montmorency* for three distinct weeks. (**D**): Deployment week, (**S**): 2021 summer solstice, (**W**) 2020 winter solstice [3].

## Context



Figure 5: Experiment during a heavy snowstorm in Quebec City, Canada [4].

# Context

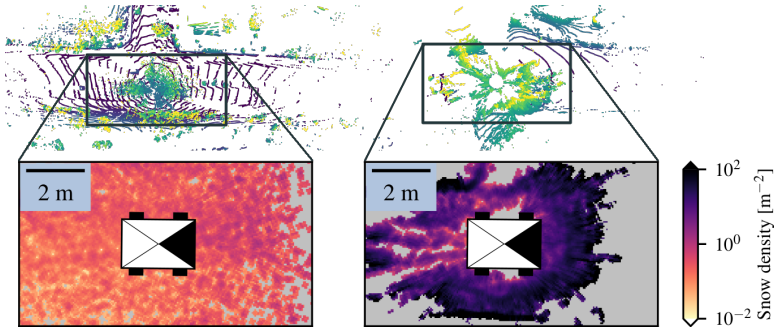


**Figure 6:** Examples of snow density fields with their associated point clouds. Left: Weak snowstorm. Right: Heavy snowstorm with a snow gust [4].

# Context

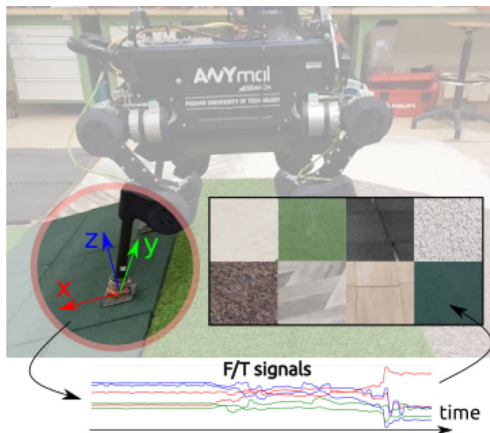


Figure 7: Haptic-based TC for legged robots [5]

# Context



Figure 8: Proprioceptive-based TC for wheeled robots [6]



# BorealTC dataset for terrain classification (TC)

- ▶ Recorded with a Husky A200 from *Clearpath Robotics* (Kitchener, Ontario, Canada).
- ▶ 116 min of proprioceptive measurements
  - ▶ Wheel service (motor currents and wheel velocities) @ 6.5 Hz.
  - ▶ Xsens MTi-30 IMU (6-DOF angular velocities and linear accelerations) @ 100 Hz.

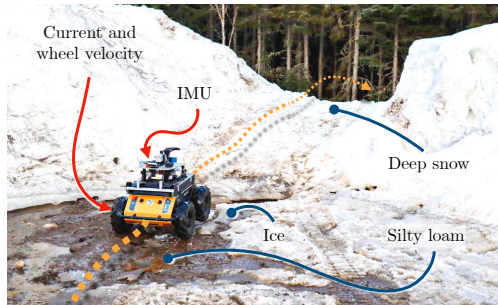


Figure 9: An example of challenges caused by terrain in boreal forests.

# Terrains considered in Boreal1TC



(a) SILTY LOAM



(b) DEEP SNOW



(c) ASPHALT



(d) FLOORING



(e) ICE

Figure 10: Types of terrains considered in our dataset.

# Our Approach

BorealTC was combined with the Vulpi dataset from Vulpi *et al.* [6]: 13 min of data on four different terrains on a experimental farm in San Cassiano 🇮🇹 .

Terrain classification was evaluated with:

- ▶ a Convolutional Neural Network (CNN) classifier [6];
- ▶ the state space model (SSM)-based Mamba architecture [7], [8].

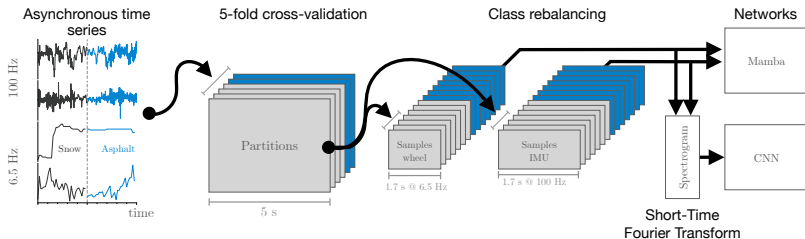


Figure 11: Overview of the training process.

# Results

## Models Performance

Table 1: Vulpi dataset (13 min).

Terrain	Precision (%)	Recall (%)	F1 score (%)	Accuracy (%)
CNN				
CONCRETE	99.21	95.27	97.20	94.12
DIRT ROAD	92.40	92.05	92.22	
PLOUGHED	96.94	98.96	97.94	
UNPLOUGHED	88.20	90.48	89.32	
Mamba				
CONCRETE	87.13	83.33	85.19	86.76
DIRT ROAD	91.34	83.90	87.46	
PLOUGHED	93.93	96.67	95.28	
UNPLOUGHED	76.08	83.93	79.81	

# Results

## Models Performance

Table 1: Vulpi dataset (13 min).

Terrain	Precision (%)	Recall (%)	F1 score (%)	Accuracy (%)
CNN				
CONCRETE	99.21	95.27	97.20	94.12
DIRT ROAD	92.40	92.05	92.22	
PLOUGHED	96.94	98.96	97.94	
UNPLOUGHED	88.20	90.48	89.32	
Mamba				
CONCRETE	87.13	83.33	85.19	86.76
DIRT ROAD	91.34	83.90	87.46	
PLOUGHED	93.93	96.67	95.28	
UNPLOUGHED	76.08	83.93	79.81	

Table 2: BorealTC dataset (116 min).

Terrain	Precision (%)	Recall (%)	F1 score (%)	Accuracy (%)
CNN				
ASPHALT	<b>92.98</b>	83.89	88.20	<b>93.96</b>
FLOORING	<b>97.29</b>	<b>98.70</b>	<b>97.99</b>	
ICE	<b>97.25</b>	<b>98.11</b>	<b>97.68</b>	
SILTY LOAM	<b>96.00</b>	<b>97.24</b>	<b>96.61</b>	
SNOW	86.84	<b>92.31</b>	89.49	
Mamba				
ASPHALT	91.90	<b>85.50</b>	<b>88.59</b>	93.68
FLOORING	95.46	98.17	96.79	
ICE	97.12	97.36	97.24	
SILTY LOAM	95.39	96.20	95.79	
SNOW	<b>88.68</b>	91.57	<b>90.10</b>	

# Results

## Train dataset size ablation study

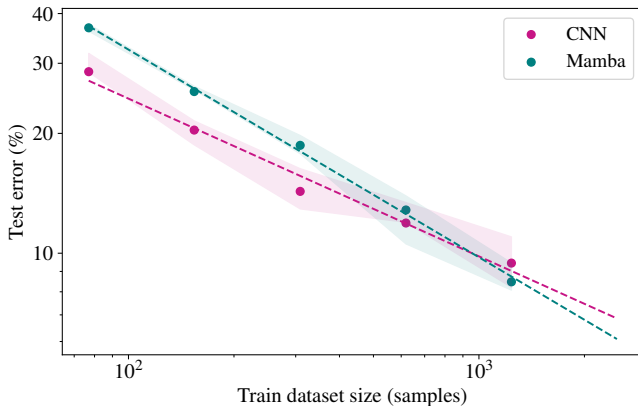
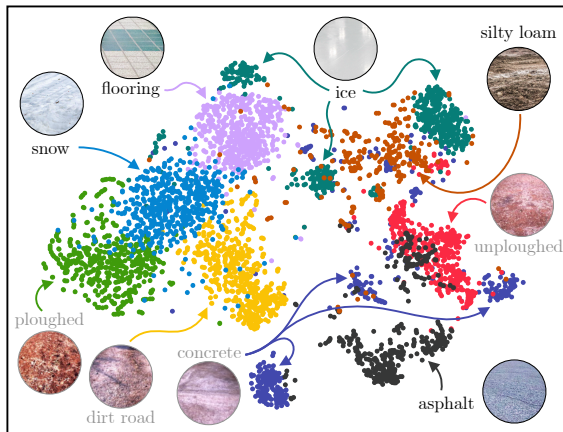


Figure 12: Influence of train dataset size on the test error in log-log scale.

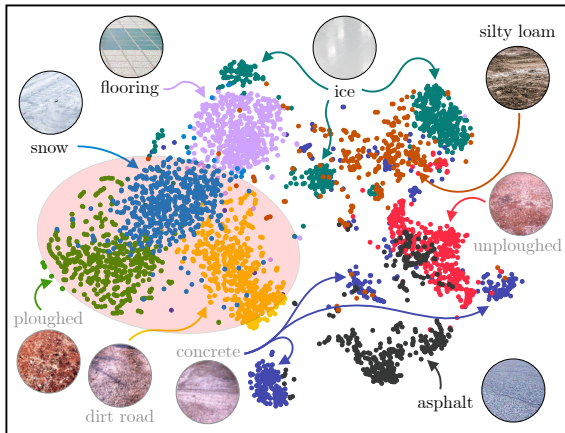
# Results

Latent space between the BorealTC and Vulpi [6] datasets



# Results

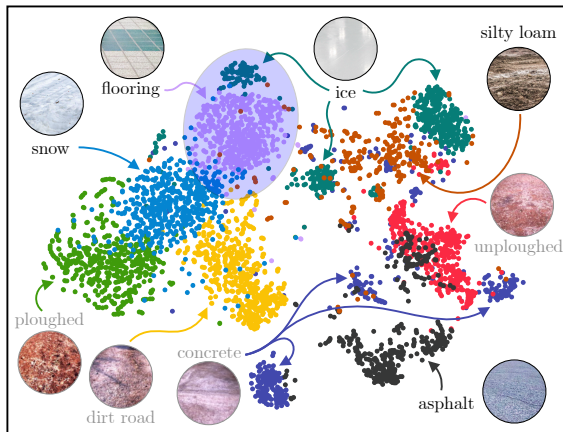
Latent space between the BorealTC and Vulpi [6] datasets





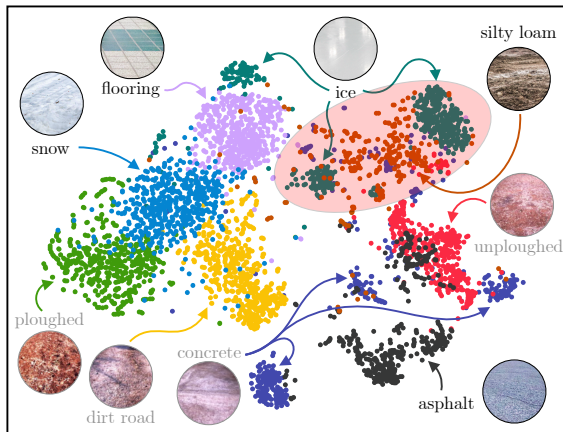
# Results

Latent space between the BorealTC and Vulpi [6] datasets



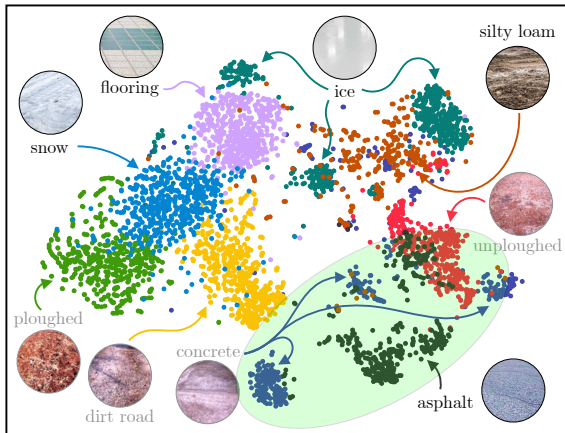
# Results

Latent space between the BorealTC and Vulpi [6] datasets



# Results

Latent space between the BorealTC and Vulpi [6] datasets



# Contributions

- ▶ BorealTC dataset for terrain classification in boreal forests.
- ▶ Improvement on CNNs methods for data-driven terrain classification.
- ▶ Exploration of SSM-based approaches for terrain classification.
- ▶ Assessment of terrain classes on a combined terrain classification dataset.

# Future Research

- ▶ Compare with other sensor modalities [9].
- ▶ Compare with other architectures.
- ▶ Extend the dataset.
  - ▶ Standardize the data acquisition procedure
  - ▶ Deploy a standard vehicle platform in various biomes
  - ▶ Combine the datasets from different vehicles
- ▶ Expand to terrain characterization [10].

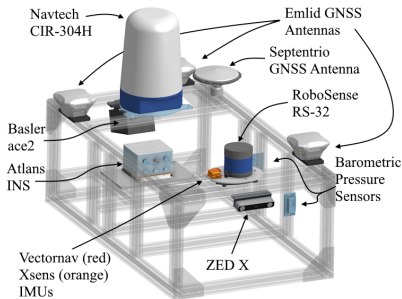


**Figure 13:** Sensor modality for the proposed *Forêt Montmorency* Dataset [9].

# References I

- [1] R. Ishikawa, R. Hachiuma, A. Kurobe, and H. Saito, "Single-modal Incremental Terrain Clustering from Self-Supervised Audio-Visual Feature Learning," in *2020 25th International Conference on Pattern Recognition (ICPR)*, IEEE, Jan. 2021.
- [2] J. Zürn, W. Burgard, and A. Valada, "Self-Supervised Visual Terrain Classification From Unsupervised Acoustic Feature Learning," *IEEE Transactions on Robotics*, vol. 37, no. 2, pp. 466–481, Apr. 2021.
- [3] D. Baril, S.-P. Deschênes, O. Gamache, *et al.*, "Kilometer-scale autonomous navigation in subarctic forests: challenges and lessons learned," *Field Robotics*, vol. 2, no. 1, pp. 16281660, Mar. 2022.
- [4] C. Courcelle, D. Baril, F. Pomerleau, and J. Laconte, "18 On the Importance of Quantifying Visibility for Autonomous Vehicles Under Extreme Precipitation," in *Towards Human-Vehicle Harmonization*. De Gruyter, Mar. 2023, pp. 239250.

## References II

- [5] M. Bednarek, M. R. Nowicki, and K. Walas, “HAPTR2: Improved Haptic Transformer for legged robots’ terrain classification,” *Robotics and Autonomous Systems*, vol. 158, p. 104 236, Dec. 2022.
- [6] F. Vulpi, A. Milella, R. Marani, and G. Reina, “Recurrent and convolutional neural networks for deep terrain classification by autonomous robots,” *Journal of Terramechanics*, vol. 96, pp. 119–131, Aug. 2021.
- [7] A. Gu and T. Dao, “Mamba: Linear-Time Sequence Modeling with Selective State Spaces,” *arXiv preprint arXiv:2312.00752*, Dec. 2023.
- [8] T. Dao and A. Gu, “Transformers are SSMS: Generalized Models and Efficient Algorithms Through Structured State Space Duality,” *arXiv preprint arXiv:2405.21060*, May 2024.
- [9] M. Boxan, A. Krawciw, E. Daum, *et al.*, “FoMo: A Proposal for a Multi-Season Dataset for Robot Navigation in Forêt Montmorency,” *presented to the 2024 ICRA Workshop on Field Robotics*, 2024.

## References III

- [10] J.-M. Fortin, O. Gamache, W. Fecteau, *et al.*, “UAV-Assisted Self-Supervised Terrain Awareness for Off-Road Navigation,” *arXiv preprint arXiv:2409.18253*, submitted for the 2025 IEEE ICRA, 2025.

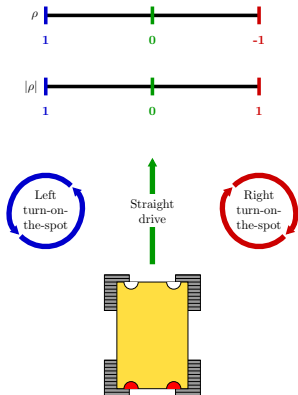


## BorealTC vs Vulpi [6] datasets

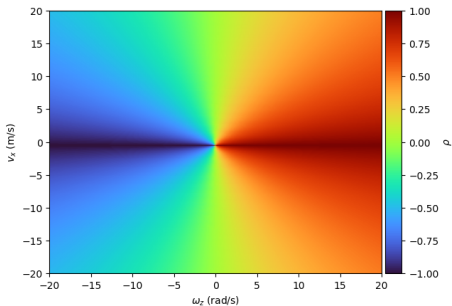
Table 3: Description of both datasets. SC: San Cassiano, FM: *Forêt Montmorency*.

Terrain	$N$	Loc.	$ \tilde{v}_x $ (IQR)	$ \tilde{\omega}_z $ (IQR)
Vulpi [6]				
CONCRETE	24	SC	0.56 (0.26)	0.00 (0.00)
DIRT ROAD	16	SC	0.56 (0.25)	0.00 (0.00)
PLOUGHED	60	SC	0.56 (0.26)	0.00 (0.00)
UNPLOUGHED	56	SC	0.56 (0.25)	0.00 (0.00)
BorealTC (ours)				
ASPHALT	111	UL	0.46 (0.58)	0.01 (0.09)
FLOORING	423	UL	0.23 (0.05)	0.02 (0.09)
ICE	450	UL	0.24 (0.38)	0.27 (0.52)
SILTY LOAM	126	FM	0.00 (0.24)	0.10 (0.17)
SNOW	281	FM	0.00 (0.31)	0.10 (0.26)

# Rotationality



$$\rho = \frac{B\omega_z}{|v_x| + B|\omega_z|}, \quad (1)$$



# Rotationality

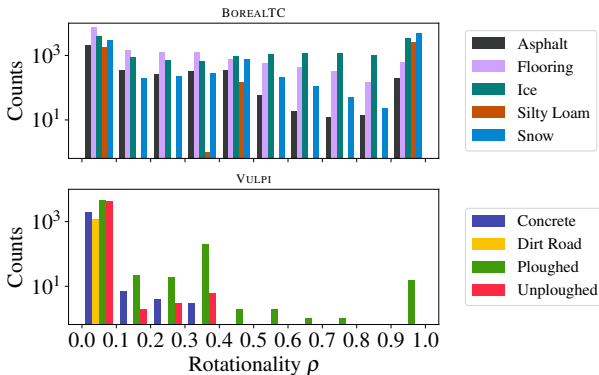


Figure 14: Distributions of rotationality of both datasets, from purely linear motions ( $\rho = 0$ ) to purely rotational motions ( $\rho = 1$ ).